Analytical Formulae for Phase Voltage RMS Squared and THD in PWM Multiphase Systems

Obrad Dordevic, *Member, IEEE*, Martin Jones, and Emil Levi, *Fellow, IEEE*

***Abstract*—The analysis and assessment of the pulse width modulation PWM techniques is commonly based on the comparison of the total harmonic distortion (THD) results. THD is usually calculated by application of the Fourier transformation and by taking a limited number of harmonics into the consideration. In this paper derivation of analytical formulae for the phase voltage THD is presented. The considered system is a symmetrical multiphase star-connected load, supplied from a multilevel pulse width modulated voltage source inverter (three-phase case is also covered). The solution is based on the Parseval's theorem, which links frequency spectrum and time domain through the average power (i.e. RMS squared value) of the signal. The assumption throughout the derivations is that the ratio of the switching to fundamental frequency is high. Derivations are based on the integration of the power of the PWM signal in a single switching period over the fundamental period of the signal. Only ideal sinusoidal reference voltages are analysed, and no injection of any type is considered. Formulae for phase voltage THD for any number of phases are derived for two- and three-level cases, for the most commonly used carrier-based methods. Comparison of the analytically obtained curves with simulation and experimental results shows a high level of agreement and validates the analysis and derivations.**

***Index Terms*—Analytical derivation, multilevel inverter, multiphase system, total harmonic distortion.**

I. Introduction

THE MOST common way of evaluating the total harmonic distortion (THD) in practice is by using the numerical approach, based on calculation of the Fourier transformation (FFT) of the signal. However, THD can be also calculated analytically, and the aim in this paper is to develop analytical formulae for the phase voltage THD. Considered system is an *n*-phase symmetrical star-connected load (e.g. induction machine) supplied from a multilevel (*l*-level) voltage source inverter (VSI). The inverter output voltage is obtained by means of the pulse width modulation (PWM).

The importance of the THD as a measure of the waveform quality is highlighted in [1], where the risk of taking a THD indiscriminately as a figure of merit is also emphasised. It is shown, using a simple example of a leg voltage, that two completely different square-waveforms can result in the same THD although the distribution of the energy in the spectrum is totally different. Hence [1] discusses some other parameters, such as weighted THD (WTHD) or normalised THD/WTHD, that are regarded as more appropriate for evaluating a signal quality. In order to define the WTHD, it is necessary to assume that all the voltage harmonics see the same inductance. This is a perfectly valid assumption in three-phase systems, but, unfortunately, it does not apply to multiphase motor drives. This is so since, when the phase number is five or more, there are two (or more) planes into which voltage harmonics map and the inductance presented to the harmonics in these planes is in general different (for example, in a five-phase induction motor drive, voltage harmonics in the first plane see an inductance that is approximately the sum of the stator and rotor leakage inductances, while harmonics mapped into the second plane see an inductance that equals only stator leakage inductance [2]). Thus, although the THD has drawbacks, it appears to be still the most appropriate indicator of the multiphase inverter output voltage quality.

It should be noted that phase voltage THD analytical formula for multilevel three-phase case operating in six-step mode is derived in [1]. The same method of integration was used in [3-5] for derivation of leg-to-leg (line-to-line) voltage THD values. Analysed waveforms are of square-wave shape rather than PWM.

The case considered in this paper is PWM operation. Analytical calculation of the PWM modulated multilevel inverter leg voltage THD has already been considered in [6, 7]. The solution given in [6] is analytical and is given for the leg voltage THD and for the WTHD (assuming the same inductance for all voltage harmonics). It has been developed for the most typical numbers of levels (two, three and five, individually for each). The research of [6] was extended in [7] with an attempt at generalisation for an arbitrary number of levels. A complete full analytical expression for the leg voltage THD for multilevel VSI supply is derived in [8].

It appears that the issue of inverter output voltage quality continues to be predominantly studied in relation to three-phase systems (e.g., [9-10]). This is in contrast to the situation related to the current ripple, which has been extensively covered in recent times for drive systems with more than three phases (e.g., [2], [11-12]). General analytical formulae for the

Manuscript received August 23, 2013; revised December 20, 2013. Accepted for publication March 31, 2014.

This paper was made possible by NPRP grant 4-152-02-053 from the Qatar National Research Fund (a member of Qatar Foundation). The statements made herein are solely the responsibility of the authors. The last author also acknowledges fruitful discussions with Dr. Alex Ruderman over the years in relation to the topic of the paper.

O. Dordevic, E. Levi, and M. Jones are with the School of Engineering, Technology and Maritime Operations, Liverpool John Moores University, Byrom Street, L3 3AF, Liverpool, UK (e-mail: o.dordevic@ljmu.ac.uk; e.levi@ljmu.ac.uk; m.jones2@ljmu.ac.uk).

phase voltage THD are therefore given in this paper for the first time. Circumstances when results are valid are explained. The same ideas of integration and derivation of the general formulae have been used in [13-15]. However, the results in [13-15] are actually not applicable to the voltage waveforms that they were aimed for.

The results arrived at in the paper can be used to compare the output voltage quality of systems with different PWM schemes, different numbers of phases and different numbers of levels. Since the inverter output voltage harmonics are responsible for additional PWM produced iron losses in electrical machines, the results are also useful for this purpose.

The paper is organised as follows. A review of the basic definitions of the signal power and THD is given in section II. Powers of various output voltages in multiphase multilevel VSIs are analysed in section III. Analytical formulae for phase voltage power in two-level and three-level multiphase VSIs are then derived in section IV. In section V, THD is calculated and obtained results are discussed and presented graphically. Analytical results are compared with simulation and experimental results in section VI. Conclusions are given in section VII.

II. Signal Power and Definition of THD

Fourier transformation is closely related to the definition of the energy and the power of the signal. The instantaneous power $p(t)$ / $p(k)$ and the energy W of the continuous/discrete signal $x(t)$ / $x(k)$ can be defined as [16]:

$$W=\int_{t_1}^{t_2} p(t)\mathrm{d}t=\int_{t_1}^{t_2}\left|x(t)\right|^2\mathrm{d}t \quad \Leftrightarrow \quad W=\sum_{k_1}^{k_2} p(k)=\sum_{k_1}^{k_2}\left|x[k]\right|^2 \quad (1)$$

where t_1 and t_2, i.e. k_1 and k_2, represent instants in time between which the energy is calculated.

For periodical signals it is very useful to define average power per signal period. The average (active) power of the continuous and discrete periodical signal is defined as:

$$P=\frac{1}{T}\int_0^T\left|x(t)\right|^2\mathrm{d}t \quad \Leftrightarrow \quad P=\frac{1}{K}\sum_{k=1}^{K}\left|x[k]\right|^2 \quad (2)$$

Since $x(t)$ and $x[k]$ are real values (measured signal), symbol for magnitude "$\left|\ \right|$" in equations (1) to (2) can be omitted and it will not be used further on.

Note that the average power in (2) represents the mean squared value of the signal. Thus the RMS value of a periodical signal can be defined as:

$$X_{rms}=\sqrt{\frac{1}{T}\int_0^T x(t)^2\mathrm{d}t}=\sqrt{P} \quad (3)$$

In other words, average power P can be defined as RMS^2.

The equation that links energy in the time and in the frequency domain is known as the Parseval's theorem. The Parseval's theorem for the periodical signal states that the energy in one period of the signal $x(t)$ (i.e. the average power P), is equal to the energy (power) in the spectrum [16]:

$$P=\frac{1}{T}\int_0^T x(t)^2\,\mathrm{d}t=\sum_{h=-\infty}^{+\infty}\left|\underline{X}_h\right|^2 \quad (4)$$

In discrete domain (4) becomes:

$$P=\frac{1}{K}\sum_{k=1}^{K}x[k]^2=\sum_{h=0}^{K-1}\left|\underline{X}_h\right|^2 \quad (5)$$

where $\underline{X}_h$ are complex values of the Fourier transformation (complex series) of the signal $x(t)$ in (4), i.e. $x[k]$ in (5).

If signal $x(t)$ (i.e. $x[k]$) is real, the spectrum will be conjugate-symmetrical [17]. Because of that, it is common in practice that instead of the full spectrum (that is symmetrical), only one half is used. To keep the same energy of the spectrum, magnitudes of the retained components have to be multiplied by $\sqrt{2}$. In this way asymmetrical spectrum with RMS values of the harmonics is obtained.

The usual way for THD calculation in practice is based on the signal spectrum and on the FFT calculation. THD is defined as a distortion of the harmonics compared to the harmonic that is of interest (useful harmonic). A dc value of the signal is usually excluded from calculation (it is not considered as distortion), and this will also be assumed here. THD of an arbitrary real but periodic signal $x[k]$ (with period T) can be calculated as:

$$\mathrm{THD}(x)=\sqrt{\frac{\sum_{h=2}^{K-2}\left|\underline{X}_h\right|^2}{2\left|\underline{X}_1\right|^2}}=\sqrt{\frac{\sum_{h=2}^{\lfloor K/2\rfloor}X_{rms,h}^2}{X_{rms,1}^2}} \quad (6)$$

where $|\underline{X}_h|$ and $X_{rms,h}$ represent magnitude in the symmetrical, i.e. RMS value in the single-sided (asymmetrical), spectrum of the h^{th} component, respectively. One can see that the THD is a square root from the ratio of the distorting power over the useful power.

THD in (6) can be expressed in a different way. If Parseval's theorem (5) for RMS values of the asymmetrical spectrum and the fact that $X_{rms}=\sqrt{P}$ from (3) are applied, (6) becomes:

$$\mathrm{THD}(x)=\sqrt{\frac{X_{rms}^2-X_{rms,1}^2}{X_{rms,1}^2}} \quad (7)$$

From (7) THD can be easily numerically calculated from the time domain without full spectrum calculation. X_{rms}^2 is the average value of the squared samples (2), (3), and the first harmonic can be calculated using a part of the FFT transformation

$$X_{rms,1}=\sqrt{2}\cdot\left|\frac{1}{K}\sum_{k=1}^{K}(x[k]\cos[\omega k]+jx[k]\sin[\omega k])\right| \quad (8)$$

where $\omega=2\pi/T$ and $\cos[\omega k]$ and $\sin[\omega k]$ represent the values of cosine/sine function at instants k when periodical signal $x[k]$ is sampled.

III. Multiphase Multilevel Output Voltage Average Powers

A. Voltage Definitions

Considered topology is a star-connected symmetrical load, Fig. 1. For the sake of generalisation, voltage values normalised with respect to the dc-bus voltage are used further on and are denoted as $u=v/V_{dc}$ (where v is a voltage in

Volts). Normalised reference voltages are assumed to be a symmetrical set of n sinusoidal signals:

$$u_{ph}^{*}(t)=\frac{m}{2}\cos\left(\omega t-\frac{2\pi}{n}(k-1)\right)$$
$$u_{LEG}^{*}(t)=\frac{1}{2}+\frac{m}{2}\cos\left(\omega t-\frac{2\pi}{n}(k-1)\right) \quad (9)$$

where $ph=a,b,c,\ldots,n$, LEG stands for the corresponding leg $LEG=A,B,C,\ldots,N$, and k is the phase/leg index $k=1$ to n. All voltages in the power circuit are referred to the negative dc-bus rail (NDC), thus 1/2 dc term in (9), Fig. 1. No injection of any type has been considered.

Phase voltage of a symmetrical load can be expressed as:

$$u_{ph}[t]=u_{LEG}[t]-u_{CMV}[t] \quad (10a)$$

where

$$u_{CMV}[t]=\frac{\sum u_{LEG}[t]}{n} \quad (10b)$$

is the common mode voltage (Fig. 1). Leg voltages $u_{LEG}[t]$ are obtained from reference leg voltages $u_{LEG}^{*}(t)$, by application of a particular PWM technique.

Further analysis is given only for the PWM methods that use two adjacent levels for creating leg voltages, and where each leg switches two times in a switching period in order to obtain reference value on average.

B. Power Definitions and Relationships

A general expression for the average power of the phase voltages, produced by the PWM multilevel multiphase inverter (including three-phase) case, will be ultimately derived in the next section. For that purpose, powers of different voltages are to be considered. These are defined as follows: $P_T(u_{ph}[t])$ is the phase voltage power, $P_T(u_{CMV}[t])$ is the common mode voltage power, and $P_T(u_{LEG}[t])$ is the leg voltage power. Symbol T in index emphasises that the average power is calculated for one period of the fundamental.

To obtain the average power of the phase voltage (10a), general expression (2) can be used:

$$P_T(u_{ph}[t])=\frac{1}{T}\int_0^T u_{ph}^2[t]\mathrm{d}t=\frac{1}{T}\int_0^T(u_{LEG}^2-2u_{LEG}u_{CMV}+u_{CMV}^2)\mathrm{d}t \quad (11)$$

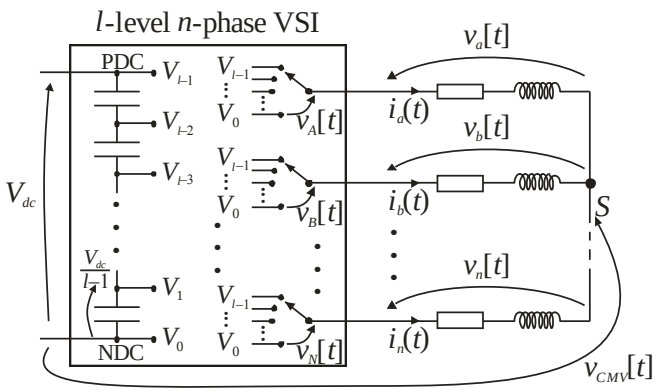

Fig. 1. Considered topology with used notation.

It can be shown (please see Appendix) that if the produced leg voltages form a symmetrical n-phase system (identical waveforms in all legs, with only the difference in the phase shift of $2\pi/n$ between consecutive legs), then $1/T\int_0^T u_{LEG}u_{CMV}\mathrm{d}t=1/T\int_0^T u_{CMV}^2\mathrm{d}t$, which is the power $P_T(u_{CMV}[t])$. The first part of the integral in (11) represents $P_T(u_{LEG}[t])$. This leads to:

$$P_T(u_{ph}[t])=P_T(u_{LEG}[t])-P_T(u_{CMV}[t]) \quad (12)$$

which represents an expected result.

The problem of finding $P_T(u_{ph}[t])$ according to (12) can be split into two tasks: calculation of $P_T(u_{LEG}[t])$, and calculation of the $P_T(u_{CMV}[t])$. Recall that the problem of determination of $P_T(u_{LEG}[t])$ has already been solved in [6-8], but here it will be shown again for the analysed cases using somewhat different approach. For calculation of $P_T(u_{CMV}[t])$ the starting point is again (2):

$$P_T(u_{CMV}[t])=\frac{1}{T}\int_0^T u_{CMV}^2\,\mathrm{d}t=\frac{\int_0^T\left(\sum_{I=A}^{N}u_I\right)^2\mathrm{d}t}{T\cdot n^2}=\frac{\sum_{I,J=A}^{N}\int_0^T u_Iu_J\,\mathrm{d}t}{T\cdot n^2} \quad (13)$$

Because of symmetry, values of $P_T(u_Iu_J)=1/T\int_0^T u_Iu_J\mathrm{d}t$ are identical for the same angular span between phases. If the phase angle between phases $2\pi/n$ is denoted with α, then the angle span between phases I,J can take discrete values of $\Lambda\alpha$, where $\Lambda=0,1,2,\ldots,\lfloor n/2\rfloor$. Finally this means that the values of $P_T(u_Iu_J)$ are mutually equal for the same Λ. For example, in the five-phase case for $\Lambda=0$, $P_T(u_Au_A)=P_T(u_Bu_B)=P_T(u_Eu_E)=\ldots=P_T(u_Iu_J,0)$; for $\Lambda=1$, $P_T(u_Au_B)=P_T(u_Bu_A)=P_T(u_Bu_C)=\ldots=P_T(u_Iu_J,1)$; and for $\Lambda=2$, $P_T(u_Au_C)=P_T(u_Cu_A)=P_T(u_Bu_D)=\ldots=P_T(u_Iu_J,2)$. Note that, if $I=J$ ($\Lambda=0$), then that term of the sum is $1/T\int_0^T u_I^2\mathrm{d}t$ and represents the power of the leg voltage $P_T(u_{LEG}[t])$. For each Λ there are exactly $2n$ pairs of I,J that have the same $P_T(u_Iu_J,\Lambda)$, except for $\Lambda=0$ and for the last $\Lambda=n/2$ for even n, for which there are n pairs of I,J with the same value of $P_T(u_{LEG})$ i.e. $P_T(u_Iu_J,n/2)$. Taking this into account, (13) can be rewritten as:

$$P_T(u_{CMV}[t])=\frac{1}{n}\sum_{\Lambda=0}^{\lfloor n/2\rfloor}K_\Lambda P_T(u_Iu_J,\Lambda) \quad (14)$$

Coefficient K_Λ in (14) is equal to 2 for every $1\le\Lambda<n/2$, while for $\Lambda=0$ and for $\Lambda=n/2$ (that exists only for even n) it is equal to $K_0=K_{n/2}=1$.

The problem of calculation of the leg, phase and common mode voltage average powers is reduced now to calculation of the $P_T(u_Iu_J)$, i.e. calculation of $P_T(u_Iu_J,\Lambda)$. $P_T(u_{LEG})$

equals $P_T(u_I u_J, \Lambda)$, for $\Lambda = 0$, while $P_T(u_{CMV})$ and $P_T(u_{ph})$ are determined by (14) and (12), respectively.

C. Determination of $P_T(u_I u_J)$

Value of $P_T(u_I u_J)$ can be calculated in a following way. Because u_I and u_J are PWM leg voltage square-waveform signals, this means that the process of integration will start with a switching period and progress with further integration throughout the whole fundamental period. The area under the product of two switching signals has to be calculated. The problem will be at first analysed in a general case, while later on the focus will be on the most typical dispositions of the carriers, in-phase disposition (PD), phase opposition disposition (POD) and alternating phase opposition disposition (APOD). An arbitrary case with two leg voltage PWM signals, u_I and u_J, within one switching period, is shown in Fig. 2.

Values of i_I, f_I and i_J, f_J in Fig. 2 are defined as:

$$\begin{aligned} i_{I,J} &= \left\lfloor u^*_{I,J}(kT_s)\cdot(l-1)\right\rfloor \\ f_{I,J} &= u^*_{I,J}(kT_s)\cdot(l-1) - i_{I,J} \end{aligned} \tag{15}$$

Integer parameter $i_{I,J}$ takes values $0, 1, 2, \ldots, (l-2)$, while fractional part is in the range $0 \le f_{I,J} < 1$. Throughout this analysis it is assumed that the voltage steps of the inverter are equal and constant.

To obtain the average power of the product of the signals u_I and u_J during one switching period, the shaded area shown in Fig. 2b has to be calculated next. The value of $P_{T_s}(u_I u_J)$ can be calculated as the total shaded area divided by the switching period T_s:

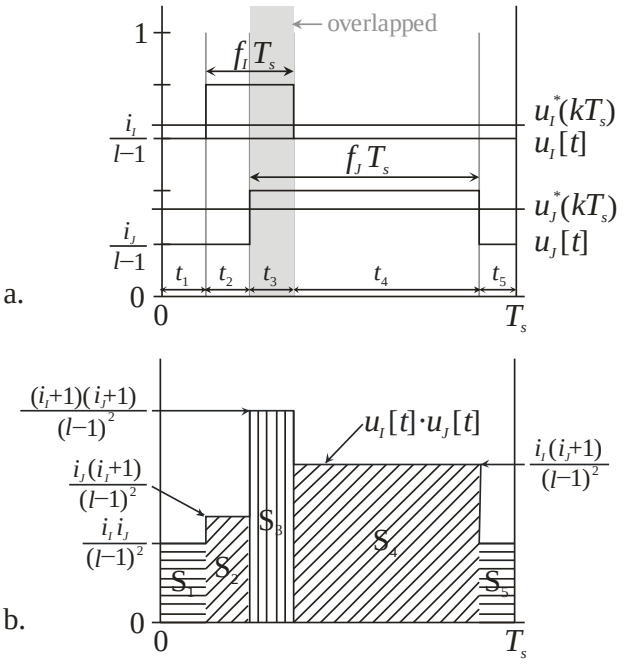

Fig. 2. Graphical interpretation of the calculation of $P_{T_s}(u_I u_J)$: a. Reference signals and produced PWM signals. b. Product of the produced PWM signals. One switching period T_s is shown.

$$\begin{aligned} P_{T_s}(u_I u_J) = \frac{1}{T_s}\sum_{k=1}^{5} S_k = \frac{1}{T_s\cdot(l-1)^2}\cdot\big(&i_I i_J t_1 + i_J(i_I+1)t_2 + \\ &+ (i_I+1)(i_J+1)\cdot t_3 + i_I(i_J+1)t_4 + i_I i_J t_5\big) \end{aligned} \tag{16}$$

Taking into account that $\sum_{k=1}^{5} t_k = T_s$, $(t_2+t_3)/T_s = f_I$ and $(t_3+t_4)/T_s = f_J$ one gets:

$$P_{T_s}(u_I u_J) = \frac{1}{(l-1)^2}(i_I i_J + i_I f_J + i_J f_I + t_3/T_s) \tag{17}$$

In (17) the last term in the sum in brackets, t_3/T_s, depends on the position of the pulses inside the switching period, i.e. on the modulation strategy. It is determined by the duration of the interval during which the pulses overlap within a switching period. Thus, in a general case, instead of t_3, a variable t_{ovl} can be used. Also, it is wise to add and subtract $f_I f_J$ term to the other terms in a bracket in (17), and replace $(i_I + f_I)/(l-1)$ and $(i_J + f_J)/(l-1)$ with u_I^* and u_J^*, respectively, see (15). Thus in general (17) can be rewritten as:

$$P_{T_s}(u_I u_J) = u_I^* \cdot u_J^* - \frac{f_I f_J}{(l-1)^2} + \frac{t_{ovl}/T_s}{(l-1)^2} \tag{18}$$

Notice here that the average power of the product of the two square-wave (PWM) signals $P_{T_s}(u_I u_J)$ is represented in a form of the power of product of the reference signals plus term that is a consequence of PWM. Also, note that the same value of $P_{T_s}(u_I u_J)$ will be obtained even if modulation strategy has multiple leg transitions within the switching period, but the duration of overlapped pulses, t_{ovl}, is the same. However, such a modulation strategy would increase switching losses and is not considered here.

Average power of the product of the signals u_I and u_J during one fundamental period, $P_T(u_I u_J)$, can be obtained as a sum, i.e. as an integral (because $f_s / f \to \infty$) of $P_{T_s}(u_I u_J)$ during one fundamental period T:

$$\begin{aligned} P_T(u_I u_J) &= \frac{1}{T}\int_0^T u_I^* u_J^*\,\mathrm{d}t - \frac{\frac{1}{T}\int_0^T f_I f_J\,\mathrm{d}t}{(l-1)^2} + \frac{\frac{1}{T}\int_0^T \frac{t_{ovl}}{T_s}\mathrm{d}t}{(l-1)^2} \\ &= P_T' + P_T'' + P_T''' \end{aligned} \tag{19}$$

As already explained, determination of the value of $P_T(u_I u_J)$ from (19) is sufficient for determination of $P_T(u_{LEG})$, $P_T(u_{CMV})$ and $P_T(u_{ph})$. Analytical formulae for two- and three-level case and for any number of phases will be derived in the following section. It should be emphasised again that only pure sinusoidal references are analysed.

IV. Multiphase Two- and Three-Level Phase Voltage Average Power

A. Two-Level Case

The first integral in (19) is independent of the number of

levels of the inverter and of the used modulation strategy. Hence, this result will be reused for the three-level case later on. Reference leg voltages are defined as in (9). Due to the symmetry, $P_T(u_I^* u_J^*, \Lambda)$ is the same for any values of I and J with the same span Λ. For the sake of calculation it will be assumed that $I = A$ while J takes value of *A*, *B*, *C*,… for different corresponding value of $\Lambda = 0,\ 1,\ 2,\ldots$ Reference signals u_I^* and u_J^* are shown in Fig. 3a. In a shown example $I = A$ and $J = B$. Substitution $\theta = \omega t$ will be used for the sake of simplicity in calculations. Because of the symmetry, this integral can be calculated as:

$$P_T^{'} = \frac{1}{2\pi}\int_0^{2\pi} u_A^* u_J^* \,\mathrm{d}\theta = \frac{2}{2\pi}\int_{\Lambda\alpha/2}^{\pi+\Lambda\alpha/2} u_A^* u_J^* \,\mathrm{d}\theta = \frac{1}{4} + \frac{m^2}{8}\cos(\Lambda\alpha) \quad (20)$$

The second integral in (19), $P_T^{''}$, is independent of the modulation strategy, but is dependent on the number of levels of the inverter. In the case of a two-level inverter, according to (15) integer values $i_{I,J}$ are always zero, thus $f_I = u_I^*$ and $f_J = u_J^*$. Because $l = 2$, this means that this integral for two-level case is again determined by the value of (20) but with the opposite sign ($P_T^{''} = -P_T^{'}$).

Now the third integral $P_T^{'''}$ of (19), with t_{ovl} term, has to be calculated. The calculation of this integral, $P_T^{'''}$, is the most complex and depends on the both number of levels and used modulation strategy. In a two-level case if both signals u_I^* and u_J^* are compared with the same carrier signal, or say in general if produced pulses are centred with respect to each other in every switching period, the solution is simple. In this case, the value of t_{ovl}/T_s is determined by the signal with a smaller fractional part, i.e. with the smaller value. Thus, taking into account that $l = 2$, and because of the symmetry,

$$P_T^{'''} = \frac{2}{2\pi}\int_{\Lambda\alpha/2}^{\pi+\Lambda\alpha/2} u_A^* \,\mathrm{d}\theta = \frac{1}{2} + \frac{m}{\pi}\sin\left(\frac{\Lambda\alpha}{2}\right) \quad (21)$$

Summation of the three components yields the value of $P_T(u_I u_J)$ of (19) for the two-level case in the form:

$$P_T(u_I u_J) = P_T^{'} + P_T^{''} + P_T^{'''} = \frac{1}{2} + \frac{m}{\pi}\sin\left(\frac{\Lambda\alpha}{2}\right) \quad (22)$$

From $P_T(u_I u_J)$, values of $P_T(u_{LEG})$, $P_T(u_{CMV})$ and $P_T(u_{ph})$ can be calculated. The value of $P_T(u_{LEG})$ in two-level case is determined as $P_T(u_I u_J, \Lambda)$, for $\Lambda = 0$:

$$P_T(u_{LEG}) = \frac{1}{2} + \frac{m}{\pi}\sin\left(\frac{0\cdot\alpha}{2}\right) = \frac{1}{2} \quad (23)$$

The value of $P_T(u_{CMV})$ can be obtained by substituting (22) into (14). Finally, an analytical solution for the phase voltage, for the two-level case and any number of phases, can be obtained by substituting (23) and obtained value for $P_T(u_{CMV})$ into (12), which leads to:

$$P_T(u_{ph}) = \frac{m}{n\pi}\sum_{\Lambda=1}^{\lfloor n/2 \rfloor} K_\Lambda \sin\frac{\Lambda\alpha}{2} \quad (24)$$

where $K_\Lambda = 2$ for every Λ, i.e. $K_\Lambda = 1$ if $\Lambda = n/2$ that exists only if n is an even number.

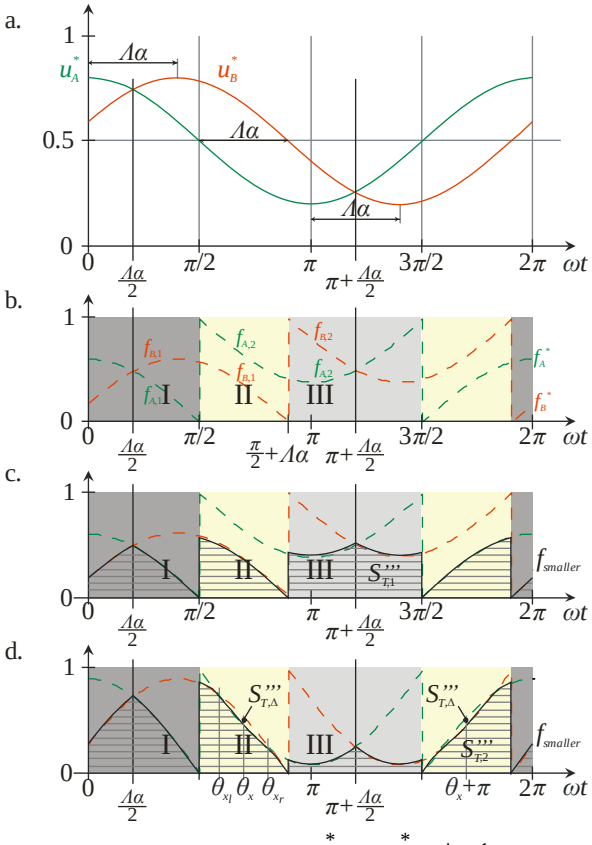

Fig. 3: a. Leg voltage reference signals u_A^* and u_B^* ($\Lambda = 1$). b. Calculation of $P_T^{''}$ term of (19) for the three-level case. Calculation of $P_T^{'''}$ term of (19) for PD-PWM: c. $f_{smaller}$ for $0 \le m \le m_x$ (29) and d. $f_{smaller}$ for $m_x < m \le 1$ (32).

B. *Three-Level PD-PWM Case*

In the three-level case calculation of the integrals in (19) is more involved. The value of $P_T^{'}$ is independent of the number of levels, thus it is determined again by (20). For the calculation of the second integral $P_T^{''}$, Fig. 3b will be used, where two fractional parts of reference signals u_A^* and u_B^* for the three-level case are shown. One can see that, because of the symmetry, it is enough to determine the value of the integral in zones I, II and III and to multiply it by 2. The value of the fractional part f_A, in zone I is $f_{A,1} = m\cos(\theta)$, while in the zones II and III it is $f_{A,2} = 1 + m\cos(\theta)$. In general, instead of leg *B*, any leg *J* can be considered ($J = A, B, C, \ldots$). The value of the fractional part of the leg *J* in zones I and II is $f_{J,1} = m\cos(\theta - \Lambda\alpha)$, while in the zone III it is $f_{J,2} = 1 + m\cos(\theta - \Lambda\alpha)$. Using this notation and by replacing $l = 3$ one gets:

$$P_T^{''} = \frac{-\frac{2}{2\pi}\left(\int_{\Lambda\alpha/2}^{\pi/2} f_{A,1} f_{J,1}\,\mathrm{d}t + \int_{\pi/2}^{\pi/2+\Lambda\alpha} f_{A,2} f_{J,1}\,\mathrm{d}t + \int_{\pi/2+\Lambda\alpha}^{\pi+\Lambda\alpha/2} f_{A,2} f_{J,2}\,\mathrm{d}t\right)}{(3-1)^2} \quad (25)$$
$$= \frac{-m^2}{8}\cos(\Lambda\alpha) + \frac{m}{2\pi}\cos(\Lambda\alpha) + \frac{\Lambda\alpha}{8\pi} - \frac{1}{8}$$

Because of the complexity of the calculation of $P_T^{'''}$, only the most typical carrier dispositions are considered, PD and POD (which is in the three-level case identical to APOD [18]). PD-PWM is considered first.

If carriers that are intersecting with reference signals u_I^* and u_J^* are denoted with c_I and c_J, then one can say that in PD-PWM case for any set of I and J, carriers c_I and c_J are always in phase. This means that PWM signals u_I and u_J are always centred with respect to each to other as in Fig. 4 (to be compared with a general case from Fig. 2). Note that this is the maximum possible value of t_{ovl}. One can see that t_{ovl}/T_s in (18) is actually determined by the signal with narrower pulse, i.e. with the signal with smaller fractional part. This will be denoted as $f_{smaller}$ ($f_{smaller} = t_{ovl}/T_s$). For calculation of $P_T^{'''}$, this means that $f_{smaller}$ has to be integrated during the whole fundamental period.

One can see that borders of integration for the small modulation index values are constant, as it is illustrated in Fig. 3c. However, when the modulation index exceeds a certain value m_x, some borders of integration ($\theta_{x_l} + k\pi$ and $\theta_{x_r} + k\pi$) become dependent on the modulation index m, Fig. 3d. Values of θ_{x_l} and θ_{x_r} in Fig. 3d can be determined in a general case for any Λ, as the crossing points of the fractional parts of $f_{A,2}$ and $f_{J,1}$. This leads to:

$$\sin\left(\theta_{x_{l,r}} - \frac{\Lambda\alpha}{2}\right) = 1/\left(2m\sin\frac{\Lambda\alpha}{2}\right) \quad (26)$$

Value of m_x corresponds to $\omega t = \theta_x$ that is determined with $\theta_{x_l} = \theta_{x_r}$. The value of θ_x can be obtained in a straightforward manner from Fig. 3, since it is in the middle of the span from $\pi/2$ to $\pi/2 + \Lambda\alpha$; thus $\theta_x = \pi/2 + \Lambda\alpha/2$. Substituting $\theta_{x_{l,r}}$ with θ_x in (26), one gets $m_x = 1/(2\sin(\Lambda\alpha/2))$.

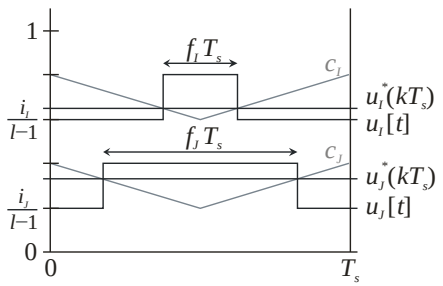

Fig. 4: Reference signals and produced PWM signals, if carriers are in phase. One switching period T_s is shown.

Taking this into account and by using (26), values of θ_{x_l} and θ_{x_r}, as a function of m, in Fig. 3d can be expressed as:

$$\theta_{x_{l,r}} = \frac{\Lambda\alpha}{2} + \arcsin\frac{m_x}{m} = \theta_x \mp \left|\arccos\frac{m_x}{m}\right| \quad (27)$$

The value of the integral $P_{T,1}^{'''}$, when $0 \le m \le m_x$, can be calculated according to the graphical interpretation shown in Fig. 3c, i.e. by dividing area of $S_{T,1}^{'''}$ by 2π. Due to the symmetry, the value of the integral of $f_{smaller}$ can be calculated (from zones I, II and III) as:

$$P_{T,1}^{'''} = \frac{1}{(l-1)^2}\frac{2}{2\pi}\left(\int_{\Lambda\alpha/2}^{\pi/2} f_{A,1}\mathrm{d}\theta + \int_{\pi/2}^{\pi/2+\Lambda\alpha} f_{J,1}\mathrm{d}\theta + \int_{\pi/2+\Lambda\alpha}^{\Lambda\alpha/2+\pi} f_{A,2}\mathrm{d}\theta\right) \quad (28)$$

One gets that:

$$P_{T,1}^{'''} = \frac{m}{2\pi}\left(1 - \sin\frac{\Lambda\alpha}{2} - \cos\Lambda\alpha\right) + \frac{1}{8} - \frac{\Lambda\alpha}{8\pi} \quad (29)$$

where $0 \le m \le m_x$.

For the higher modulation index values $m_x < m \le 1$ value of the integral $P_{T,2}^{'''}$ can be calculated directly by integration of the area $S_{T,2}^{'''}$ in Fig. 3d, and by dividing by 2π. However, it can be also calculated in a simpler way using previously obtained expression (29). One can see from Fig. 3d that $S_{T,2}^{'''} = S_{T,1}^{'''} - 2S_{T,\Delta}^{'''}$, i.e. after dividing by 2π, that $P_{T,2}^{'''} = P_{T,1}^{'''} - 2P_{T,\Delta}^{'''}$. Here $P_{T,1}^{'''}$ is as in (29), but now calculated for $m_x < m \le 1$. The value of $P_{T,\Delta}^{'''}$ for any value of Λ is:

$$P_{T,\Delta}^{'''} = \frac{1}{(l-1)^2}\frac{1}{2\pi}\int_{\theta_{x_l}}^{\theta_{x_r}} (f_{J,1} - f_{A,2})\mathrm{d}\theta \quad (30)$$

where values of θ_{x_l} and θ_{x_r} are given by (27). After calculation of the integral one gets:

$$P_{T,\Delta}^{'''} = \frac{1}{4\pi}\left(\sqrt{\frac{m^2}{m_x^2} - 1} - \left|\arccos\frac{m_x}{m}\right|\right) \quad (31)$$

Finally, to complete the set of equations, one recalls that:

$$P_{T,2}^{'''} = P_{T,1}^{'''} - 2P_{T,\Delta}^{'''} \quad (32)$$

where $P_{T,1}^{'''}$ is determined by (29), $P_{T,\Delta}^{'''}$ is given by (31), while $m_x < m \le 1$ ($m_x = 1/(2\sin(\Lambda\alpha/2))$).

For determination of $P_T(u_I u_J, \Lambda)$ in (19) values of $P_T^{'}$, $P_T^{''}$ and $P_T^{'''}$ should be replaced with values from (20), (25) and (29) for $0 \le m \le m_x$, i.e. (32) for $m_x < m \le 1$, respectively. After all the substitutions one gets ($m_x = 1/(2\sin(\Lambda\alpha/2))$):

$$P_T(u_I u_J) = \frac{1}{4} + \frac{m}{2\pi}\left(1 - \sin\frac{\Lambda\alpha}{2}\right) - \begin{cases} 0 & , 0 \le m \le m_x \\ 2P_{T,\Delta}^{'''} & , m_x < m \le 1 \end{cases} \quad (33)$$

where $P_{T,\Delta}^{'''}$ is determined by (31).

An analytical solution can be obtained now for leg, CMV and phase voltage for the three-level case with PD-PWM for

any number of phases. The value of $P_T(u_{LEG})$ is determined as $P_T(u_I u_J, \Lambda)$, for $\Lambda = 0$. Note that the last term in the sum in (33) is always 0, because $m_x \to \infty$ i.e. $m_x > 1$. One gets:

$$P_T(u_{LEG}) = \frac{1}{4} + \frac{m}{2\pi} \tag{34}$$

The value of $P_T(u_{CMV})$ can be obtained by replacing (33) into (14). Finally, after substitution of these results into (12), $P_T(u_{ph})$ for the three-level *n*-phase PD-PWM case becomes:

$$P_T(u_{ph}) = \frac{1}{2n\pi} \sum_{\Lambda=1}^{\lfloor n/2 \rfloor} \left(K_\Lambda m \sin\frac{\Lambda\alpha}{2} + \right. \\ \left. + \begin{cases} 0 & , 0 \le m \le m_x \\ K_\Lambda \left(\sqrt{\frac{m^2}{m_x^2} - 1} - \left| \arccos\frac{m_x}{m} \right| \right) & , m_x < m \le 1 \end{cases} \right) \tag{35}$$

where $m_x = 1/(2\sin(\Lambda\alpha/2))$ and $K_\Lambda = 2$ for $1 \le \Lambda < n/2$, i.e. $K_\Lambda = 1$ for $\Lambda = n/2$ (this exists only for even n). Note that m_x depends on the value of Λ; thus each value in the summation has to be calculated first.

C. Three-Level (A)POD-PWM Case

The situation when carriers c_I and c_J are in counter-phase in a particular switching period is shown in Fig. 5. One can see that two cases with a different t_{ovl} have to be considered, when $f_I + f_J \le 1$ (Fig. 5a) and when $f_I + f_J > 1$ (Fig. 5b). One gets that:

$$P'''_{T_s} = \frac{1}{(l-1)^2} \cdot \begin{cases} 0 & , f_I + f_J \le 1 \\ (f_I + f_J - 1) & , f_I + f_J > 1 \end{cases} \tag{36}$$

where P'''_{T_s} represents $t_{ovl}/(T_s \cdot (l-1)^2)$ term from (18).

As when the carriers are in phase, the expression (36) has to be integrated during the fundamental period to obtain P'''_T. Here some care has to be exercised. Most frequently signals u_I^* and u_J^* do not belong to the carriers that are in counter-phase during the whole fundamental period, Fig. 6. This means that in some intervals, when references belong to the carriers that are in phase, or to the same carrier, $f_{smaller}$ has to be integrated for determination of P'''_T (zones I and III). When references are compared with carriers that are in counter-phase and if $f_I + f_J \le 1$, the value for integration is 0 (upper row in (36); zone II, the second half), i.e. if $f_I + f_J > 1$, $f_I + f_J - 1$ (lower row in (36); zone II, the first half), has to be integrated for determination of P'''_T.

In the shown example shaded area in Fig. 6b shaded area represents the last integral in (19). Because of symmetry, it can be calculated in general case as:

$$P'''_T = \frac{1}{4\pi} \left(\int_{\Lambda\alpha/2}^{\pi/2} f_{A,1} \mathrm{d}\theta + \int_{\pi/2}^{\pi/2+\Lambda\alpha/2} (f_{A,2} + f_{J,1} - 1) \mathrm{d}\theta + \int_{\pi/2+\Lambda\alpha}^{\pi+\Lambda\alpha/2} f_{A,2} \mathrm{d}\theta \right) \tag{37}$$

One can see that the borders of integration are not changing with the increase of the modulation index *m*. This simplifies integration. After calculation of the integral one gets:

$$P'''_T = \frac{m}{2\pi} \left(\cos\frac{\Lambda\alpha}{2} - \sin\frac{\Lambda\alpha}{2} - \cos\Lambda\alpha \right) + \frac{1}{8} - \frac{\Lambda\alpha}{8\pi} \tag{38}$$

As already mentioned, there is no change of the borders of integration, so (38) is valid for the whole modulation index range of m from 0 to 1. Similarity of (38) with the corresponding expression (29) (that is only valid for $m < m_x$) for the PD-PWM is obvious.

The value of $P_T(u_I u_J, \Lambda)$, for any Λ, for (A)POD-PWM case can be calculated next. It is determined by a sum of terms, as in (19), where P'_T and P''_T are given with (20) and (25), respectively, and P'''_T is now defined by (38). After substitutions one gets:

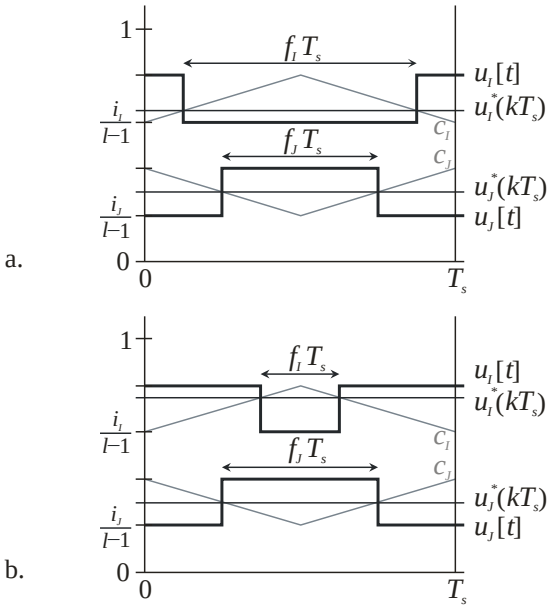

Fig. 5: Reference signals and produced PWM signals, if carriers are in counter-phase if: a. $f_I + f_J \le 1$, b. $f_I + f_J > 1$. One switching period T_s is shown.

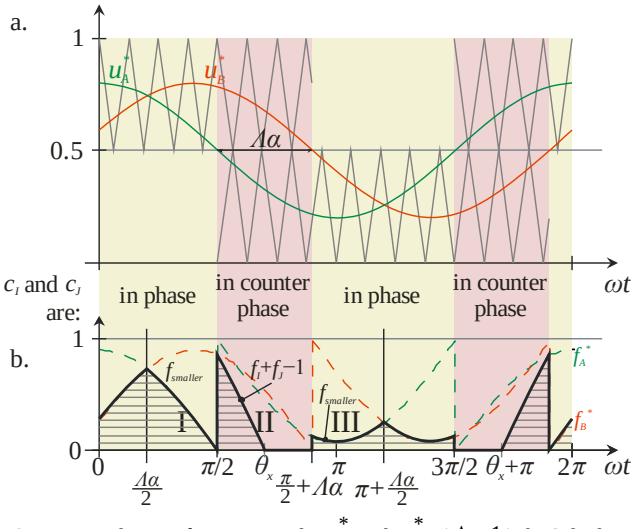

Fig. 6: a. Leg voltage reference signals u_A^* and u_B^* ($\Lambda = 1$). b. Calculation of P'''_T term of (19) for (A)POD-PWM represents a combination of (29) and (36) when carriers are in phase and in counter phase.

$$P_T(u_I u_J) = \frac{1}{4} + \frac{m}{2\pi}\left(\cos\frac{\Lambda\alpha}{2} - \sin\frac{\Lambda\alpha}{2}\right) \quad (39)$$

An analytical solution can be now obtained for the leg, phase and CMV voltage for the three-level case with (A)POD carrier disposition, for an *n*-phase system. As explained, the value of $P_T(u_{LEG})$ is determined as $P_T(u_I u_J, \Lambda)$, for $\Lambda = 0$. One gets that $P_T(u_{LEG})$ is the same as in PD-PWM case, i.e. that it is again determined with (34). This result can be generalised: $P_T(u_{LEG})$ is independent of a modulation strategy, provided that f_s / f is high enough, the output leg step is constant, and only two adjacent levels are used (see [8]).

The value of $P_T(u_{CMV})$ can be obtained by substituting (39) into (14). After substitution of all these results into (12), $P_T(u_{ph})$ for the three-level *n*-phase case with carriers in (A)POD becomes:

$$P_T(u_{ph}) = \frac{m}{2n\pi}\left(n - 1 - \sum_{\Lambda=1}^{\lfloor n/2 \rfloor} K_\Lambda \left(\cos\frac{\Lambda\pi}{n} - \sin\frac{\Lambda\pi}{n}\right)\right) \quad (40)$$

where $K_\Lambda = 2$ for $1 \le \Lambda < n/2$, i.e. $K_\Lambda = 1$ for $\Lambda = n/2$ (which exists only for even n). Note that the power of the produced phase voltage is linearly proportional to the value of the modulation index *m*, with the coefficient of proportionality being different for the different numbers of phases n. Linear dependence was also present in the two-level case (24), while in the three-level case with PD-PWM (35) the dependence was more complex.

V. Analysis and Graphical Representation of Phase Voltage Power and THD

Comparing (34) with (23) one can see that the power of the leg voltage signal created by the three-level inverter is always lower than power produced by the two-level inverter $(1/4 + m/(2\pi) < 1/2, 0 \le m \le 1)$. However, this power is always greater or equal than the power of the ideal sinusoidal leg voltage reference of (9), that can be calculated by (2) and that amounts to $1/4 + m^2/8$. This means that if a multilevel inverter is used, 'wasted' power that goes into the additional non-fundamental harmonics is reduced compared to the two-level case. Usage of non-adjacent levels in a three-level inverter causes two-level operation. Thus one can conclude that usage of non-adjacent levels will increase 'wasted' power, which confirms previously given statement.

From the previous analysis one can see that the position of pulses inside the switching period T_s, i.e. used modulation strategy, is important for determination of the power of the phase voltages but not for the leg voltages. For different position of pulses different area under $u_I u_J$ curve, i.e. $P_{T_s}(u_I u_J)$, can be obtained, see (18) and Fig. 2. In fact this difference is determined by the t_{ovl}. If the carriers are in phase (Fig. 4), then the area, i.e. the value of $P_{T_s}(u_I u_J)$, is greater than if the carriers are in counter-phase, Fig. 5 (proof: $f_{smaller} = \min(f_I, f_J) > f_I + f_J - 1$ for $0 \le f_I, f_J < 1$). This is also obvious since t_{ovl} is greater for PD than in (A)POD case. A consequence of this is that after integration over the fundamental period the obtained value of $P_T(u_I u_J)$ will be greater for PD-PWM than for POD- or APOD-PWM for any pair of I and J. Referring this back to (14), this means that PD-PWM will put more power into CMV than (A)POD. Because $P_T(u_{LEG})$ is the same for PD and (A)POD (34), looking at (12) this means that PD-PWM produced phase voltages will contain less power than those produced by POD and APOD carrier dispositions. This is in agreement with conclusions of [18], where double Fourier transformation analysis of the leg voltages has been done. It was shown that PD-PWM localises high amount of energy at the multiples of the switching frequency and, since those harmonics cancel in phase voltages, PD-PWM has been proposed as superior when compared to the POD and APOD. The same conclusion is obtained here through the time domain analysis, and through the spectral analysis in [18], thanks to the Parseval's theorem (5) that links a signal power in the time and in spectral domains.

If reduction of the power that is going into CMV is of interest, then the (A)POD represents the best choice. Further, one can see that (40) for even numbers of phases *n* becomes equal to $P_T(u_{ph}) = m/(2\pi)$. Comparing this result with the power of the leg voltage (34), for the three-level case, one can see that the only difference is in the constant term 1/4. This power is the power of dc value of 1/2 that is a difference of reference phase and reference leg voltages that are referred to NDC. This means that for an even *n* and for the three-level inverters with carriers in (A)POD the CMV does not contain any ripple and is a pure dc-value (of $1/2 \cdot V_{dc}$) or zero, depending on the point to which it is referenced. Because of the mirror-symmetry around the time axis, this conclusion can be generalised to any even number of phases with an odd number of levels, and to both POD and APOD carriers.

Because PD-PWM has the maximum possible t_{ovl} in each switching period, one can generalise that it puts the maximum power into common mode voltage, and minimises power that goes into the phase voltage, i.e. RMS[2]. As a consequence, one can conclude that PD-PWM is a modulation strategy that produces the lowest phase voltage THD, see (7).

Phase voltage power, according to the analytical expressions (24), (35) and (40) for the two- and three-level case with PD and (A)POD carrier dispositions, respectively, and for phase numbers $n = 3, 5, 6$ and 7 is shown graphically in Fig. 7. Power of the reference phase voltages, given with (9), can be easily calculated using (2) and is also shown in Fig. 7 (gray dashed line, $P_T(u_{ph}^*) = m^2/8$).

Fig. 7 clarifies the previously given statement, that the phase voltage produced by the PD-PWM has a smaller average power (smaller higher order harmonics) than the voltage produced by the (A)POD-PWM for the same number of phases. Of course, phase voltage produced by the (A)POD-PWM has a smaller average power than the one produced by

the two-level PWM inverter. An interesting fact to be noted is that the phase voltage produced by a three-phase inverter has smaller power than those produced by inverters with higher numbers of phases. For the two-level case and for three-level case with PD-PWM this can be generalised into a statement that power of the phase voltage increases with the phase number *n*; however, for (A)POD this is not the case.

Note that the values for the three-level PD-PWM in Fig. 7 are twice smaller than for the two-level case for the given number of phases, for small modulation index values. This is also obvious from equations (24) and (35). The maximum value of the modulation index m up to which this applies is determined by the smallest value of m_x for a particular *n*, i.e. by $\min(1/(2\sin(\Lambda\pi/n)))$. Thus for the three-phase case this is true up to the modulation index of 0.5774, for the five-phase case up to 0.5257, for the six-phase case up to 0.5, and for the seven-phase case up to 0.5129.

Operation of the three-level inverter with PD carrier disposition for small modulation index values is similar to the operation of the two-level VSI with halved dc-bus voltage. From the point of view of the space vectors and sub-sectors, used space vectors for sub-sectors of the three-level case are identical for the small modulation index values as for the two-level case with halved dc-bus value. Maximum modulation index in the linear modulation region for an *n*-phase system, for odd numbers of phases, is given with $m_{max}=1/\cos(\pi/(2n))$ [19], and it is obtained with min-max zero-sequence injection. For even numbers of phases m_{max}=1 and linear region cannot be extended. Particular values of the modulation index m_x, up to which the power of the phase voltage obtained with the two-level inverter is twice more than the power obtained with the three-level inverter (0.5774, 0.5257, etc.), are equal to $m_{max}/2$ for any particular number of phases.

By using analytical expressions (24), (35) and (40) for the phase voltage average power obtained with two- and three-level multiphase PWM inverter with PD and (A)POD carriers,

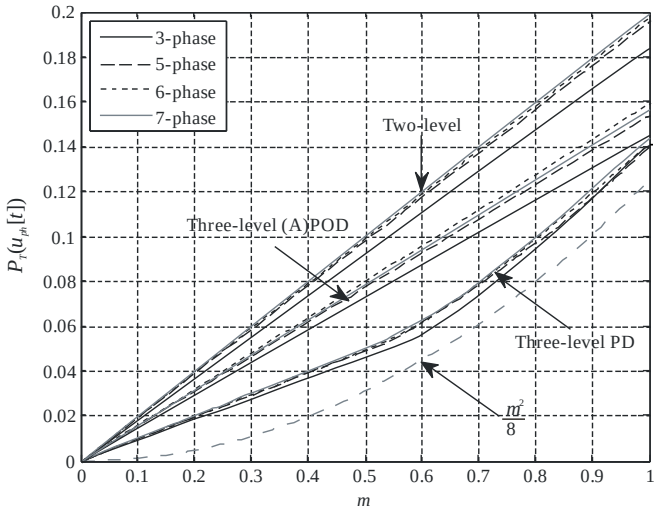

Fig. 7: Analytical curves plotted using (24), (35) and (40): the average power during the fundamental period of the phase voltage generated by two- and three-level PWM multiphase inverters with PD and (A)POD carriers, $P_T(u_{ph})$.

and by using (7), THD values of the phase voltages can be obtained. According to (3), RMS values of the phase voltages can be calculated as $U_{ph,rms}=\sqrt{P_T(u_{ph})}$. Total harmonic distortion is defined with reference to the fundamental (first harmonic) of the output, which is equal to the reference value since dead time has not been considered. RMS value of the fundamental is equal to $U_{ph,rms,1}=\sqrt{P_T(u_{ph}^*)}=m/(2\sqrt{2})$. Substituting these expressions into (7), one gets:

$$\mathrm{THD}_T(u_{ph})=\frac{\sqrt{P_T(u_{ph})-P_T(u_{ph}^*)}}{U_{ph,rms,1}}=\sqrt{\frac{8P_T(u_{ph})}{m^2}-1} \quad (41)$$

where $P_T(u_{ph})$ is given by (24), (35) and (40) for the considered cases of the two-level and three-level PWM with PD and (A)POD carriers, respectively, and m is the modulation index value $0\le m\le 1$.

Curves that represent THD of the phase voltages, for the two-level and three-level PWM with PD and with (A)POD carriers, are generated according to the analytical expression (41) for various phase numbers and are shown in Fig. 8.

Calculation of the phase voltage power and THD for any other number of levels and any other shape of references can be executed in the same manner. However, due to complex analytical calculations and due to the simplicity of finding the problem solution numerically, full solution for only the most common cases in practice, two-level and three-level PD and (A)POD PWM, was given here. Numerical calculation of the THD does not necessarily mean calculation by finding the spectrum first; THD can be also calculated numerically in time domain, as explained at the end of section II. Some results for the phase voltage THD, for the three-phase load supplied from the five, seven and nine-level inverter with different carrier-based strategies, are given in [20], where the region of overmodulation is also covered. The method of THD calculation in [20] was obviously numerical, by means of the spectrum determination; however the number of harmonics taken into consideration is not given.

VI. Comparison of the Theoretical Curves with Simulation and Experimental Results

To validate the theoretically obtained analytical results, simulations and experiments have been done. Simulation software PLECS block-set has been used. Scope in this software has a built-in function for RMS and THD calculation. The built-in functions use exact numerical approach as the one described in section II, but are also adapted to work with a variable simulation step time [21]. According to (3) average power of the signals is calculated as a squared value of the RMS value from the PLECS scope. This way of calculation is very precise and that is the reason why this software has been used for proper simulation verification of analytical results.

Theoretical analytical curves for power of the generated output phase voltage of Fig. 7 are compared with simulation values from PLECS scope (RMS^2) in Fig. 9. A corresponding comparison of the analytical THD traces with simulation results, which are the values read from the PLECS scope, is shown in Fig. 10. Simulations are done for the constant *V/f*

ratio ($m/f = 1/50$), for V_{dc}=1 V (for easier comparison of power curves, when needed), and for the switching frequency of $f_s = 2$ kHz. Dead time has been neglected. Excellent agreement between simulation and analytical results is obvious. This means that the used switching frequency, i.e. ratio f_s/f, is high enough for all the modulation indices.

In experiments, as in simulations, V/f ratio was kept constant and equal to $m/f = 1/50$ and $f_s = 2$ kHz. Custom-made two-level and three-level inverter of the neutral-point clamped (NPC) type were used. Two-level inverter can supply up to an eight-phase system. Three six-pack Infineon IGBT modules FS50R12KE3 are used. IGBT modules of the three-level NPC inverters are Semikron SKM50GB12T4, while clamping diodes are Semikron SKKD 46/12. Each NPC inverter has six phases, so that for seven-phase experiments two units were paralleled to the same dc-bus. The experiments have been done using three-, five-, and six-phase symmetrical induction machines and for seven-phase case using symmetrical $R-L$ load. Dc voltage, provided from Sorensen SGI 600/25 dc source, was 600V in all the cases, except for the six-phase machine where it had to be lowered to 250 V due to the limitation imposed by the voltage rating of the machine. The inverters' dead time is 6 μs. THD was calculated using Fourier transformation as in (6). Two cases were considered: when the harmonic spectrum was limited at 21 kHz (the first ten side-bands), and when a full spectrum is used for calculation of THD. Comparison of theoretical analytical curves and experimental results for the THD is given in Fig. 11.

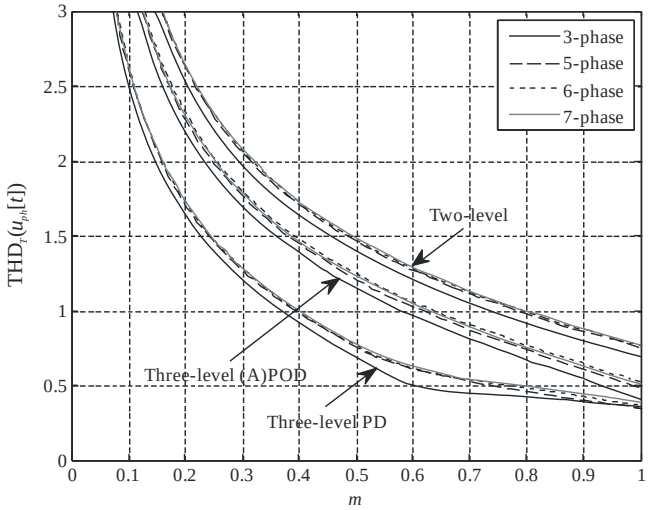

Fig. 8: THD, as given by the analytical expressions (41), for the generated output phase voltage of the two- and three-level PWM multiphase inverters, $\mathrm{THD}_T(u_{ph})$.

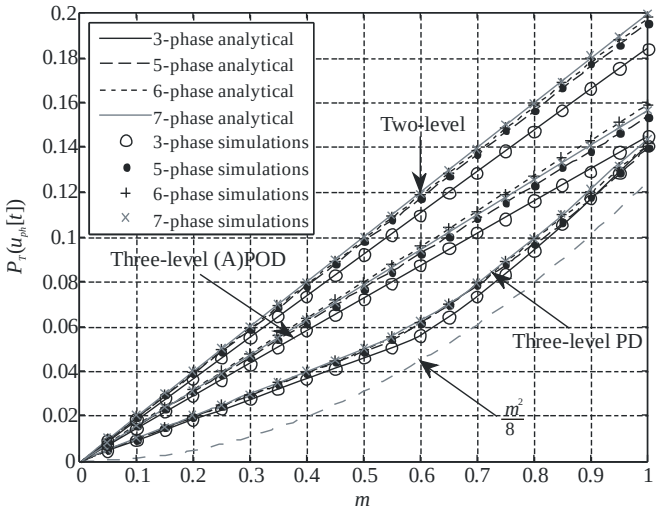

Fig. 9: Comparison of the analytical curves for the average power of the phase voltage generated by two- and three-level PWM multiphase inverter (Fig. 7; continuous lines) with simulation results from PLECS scope RMS^2 (discrete values, identified with markers).

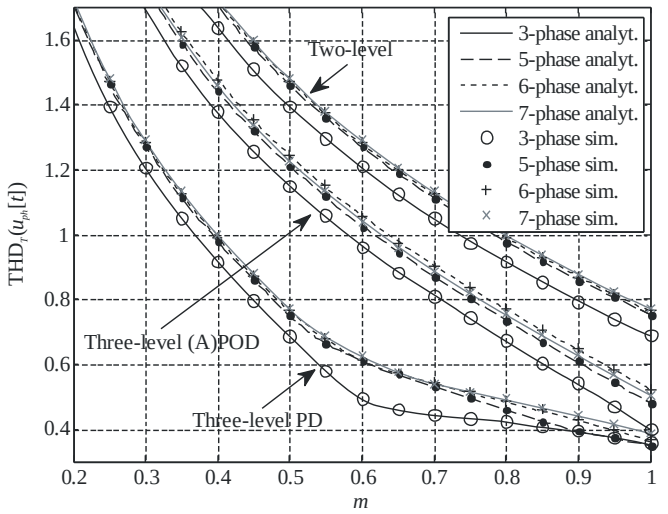

Fig. 10: Comparison of the analytical curves for phase voltage THD (Fig. 8; continuous lines) with simulation results from PLECS scope (discrete values, identified with markers).

From Fig. 11, it is evident that there are minor differences between the experimental and analytical values. With full spectrum, experimental THD values are slightly higher than analytical predictions. This is due to the dead-time effect, which has not been considered in either analytical derivations or in simulations but is unavoidable in practice. The effect of truncating the spectrum at 21kHz is also evident in Fig. 11. With the applied truncating, all the experimental THD values become slightly lower than the theoretically predicted values, regardless of the existence of the dead time.

Finally, an attempt is made to evaluate the minimum switching to fundamental frequency ratio that is required for the procedure in the paper to be regarded as accurate enough. The highest fundamental frequency (50Hz here) is used and phase voltage THDs are evaluated for all the considered (two-level and three-level) PWM schemes, using at first analytical expressions. Simulations are further done for switching frequencies 2kHz, 1kHz and 500Hz, for all the considered phase numbers. Table I shows percentage difference between the value at the used switching frequency and the analytical value. It follows from Table I that the f_s/f ratio of 40 (i.e. 2kHz switching frequency) is more than sufficiently high to provide accurate results. Even the ratio of just 20 (i.e. 1kHz) appears as high enough for the two-level and three-level (A)POD PWM for all phase numbers. However, reducing the ratio to only 10 does lead to rather high differences and this ratio is therefore too low.

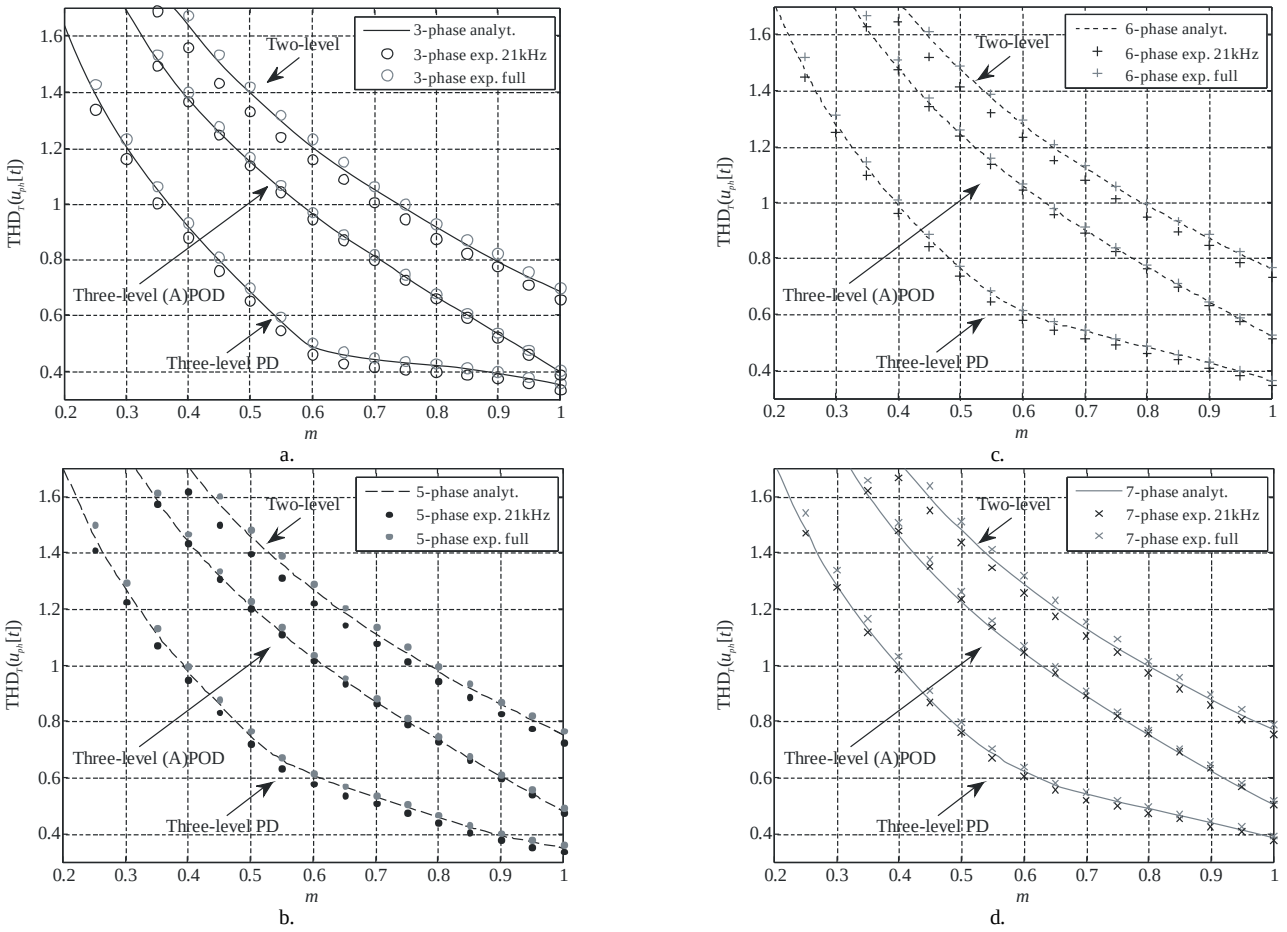

Fig. 11: Comparison of the analytical curves (continuous lines) for the phase voltage THD (Fig. 8) with experimental results using the full and up to 21kHz spectrum for THD calculation (discrete values labelled with corresponding markers), for a. three-, b. five-, c. six- and d. seven-phase configuration.

TABLE I. PERCENTAGE DIFFERENCE BETWEEN THE PHASE VOLTAGE THD VALUE AT A GIVEN SWITCHING FREQUENCY AND THE VALUE OBTAINED USING ANALYTICAL EXPRESSION. FUNDAMENTAL FREQUENCY IS 50HZ IN ALL CASES.

f_s	2kHz				1kHz				500Hz			
Phase no.	3	5	6	7	3	5	6	7	3	5	6	7
2-level	0.5	0	0.3	0.4	2.2	-0.1	1.1	1.3	8.7	-0.4	6.4	5
3-level PD	1.9	0.7	1.3	0.5	7.9	1.3	5.6	2.3	30	2.2	25.2	13
3-level (A)POD	0.4	-0.1	-0.1	0.2	1.6	-0.6	-0.5	-0.1	17.9	2.5	9.4	11.2

VII. CONCLUSION

Analytical expressions for the average power (RMS^2) and THD for the PWM produced phase voltage are derived in this paper. Considered reference voltage is purely sinusoidal, and analysis is given for the star-connected symmetrical load. Due to the complexity of the analytical derivation, and simultaneous simplicity in obtaining the results numerically, the analysis has been restricted to the two- and three-level *n* phase cases. However, the principle used is general and it can be applied to any number of levels and phases. For the three-level case PD-PWM and POD (i.e. APOD) PWM are covered. The superiority of the PD-PWM, for producing phase voltages with lower THD, is confirmed once again by the time domain power analysis here. Analytical curves are compared with simulation and experimental results, and an excellent agreement is demonstrated.

APPENDIX

A proof of the identity

$$\frac{1}{T}\int_0^T u_{LEG}u_{CMV}\,\mathrm{d}t \Leftrightarrow \frac{1}{T}\int_0^T u_{CMV}^2\,\mathrm{d}t \qquad (42)$$

is provided here. Let us select u_A as a representative of u_{LEG} and n=5, without any loss of generality. Then

$$\frac{1}{T}\int_0^T u_A\frac{u_A+\ldots+u_E}{5}\,\mathrm{d}t \Leftrightarrow \frac{1}{T}\int_0^T \frac{(u_A+\ldots+u_E)^2}{5^2}\,\mathrm{d}t \qquad (43)$$

Thus one has an identity of the functions to be integrated,

$$\frac{u_A^2+\ldots+u_Au_E}{5} \Leftrightarrow \frac{u_A^2+\ldots+u_E^2+2u_Au_B+2u_Au_C+\ldots}{5^2} \qquad (44)$$

Because of the symmetry, all integrals with the same angular span between phases (*A-A*, *B-B*, …, *E-E*; *A-B*, *B-C*, …, *E-A*; *A-C*, *B-D*, …, *E-B*) are identical, so that one can write

$$\frac{u_A^2+2u_Au_B+2u_Au_C}{5} \Leftrightarrow \frac{5u_A^2+10u_Au_B+10u_Au_C}{5^2} \qquad (45)$$

This concludes the proof of the validity of (42).

REFERENCES

[1] D. G. Holmes, T. A. Lipo, "*Pulse width modulation for power converters: principles and practice*," IEEE Press, Piscataway, NJ, 2003.
[2] D. Dujic, M. Jones, E. Levi, "Analysis of output current ripple RMS in multi-phase drives using space vector approach," *IEEE Trans. on Power Electronics*, vol. 24, no. 8, pp. 1926-1938, 2009.
[3] N. Farokhnia, H. Vadizadeh, S. H. Fathi, F. Anvariasl, "Calculating the formula of line-voltage THD in multilevel inverter with unequal DC sources," *IEEE Trans. on Industrial Electronics*, vol. 58, no. 8, pp. 3359-3372, 2011.
[4] N. Yousefpoor, S. H. Fathi, N. Farokhnia, H. A. Abyaneh, "THD minimization applied directly on the line-to-line voltage of multilevel inverters," *IEEE Trans. on Industrial Electronics*, vol. 59, no. 1, pp. 373-380, 2012.
[5] N. Farokhnia, S. H. Fathi, N. Yousefpoor, M. K. Bakhshizadeh, "Minimisation of total harmonic distortion in a cascaded multilevel inverter by regulating voltages of dc sources," *IET Power Electronics*, vol. 5, no. 1, pp. 106-114, 2011.
[6] H. W. Van Der Broeck, "Analytical calculation of the harmonic effects of single phase multilevel PWM inverters," in *Proc. IEEE Industrial Electronics Society Annual Conf. IECON*, Roanoke, VA, 2003, pp. 243-248.
[7] J. I. Leon, L. G. Franquelo, E. Galvan, M. M. Prats, J. M. Carrasco, "Generalized analytical approach of the calculation of the harmonic effects of single phase multilevel PWM inverters," in *Proc. IEEE Industrial Electronics Society Annual Conf. IECON*, Busan, South Korea, 2004, pp. 1658-1663.
[8] O. Dordevic, M. Jones, E. Levi, "Analytical formula for leg voltage THD of PWM multilevel inverter, " in *Proc. IET Int. Conf. on Power Electronics, Machines and Drives PEMD*, Manchester, UK, 2014 (accepted).
[9] D. J. Kostic, Z. Z. Avramovic, N. T. Ciric, "A new approach to theoretical analysis of harmonic content of PWM waveforms of single- and multiple-frequency modulators," *IEEE Trans. on Power Electronics*, vol. 28, no. 10, pp. 4557-4567, 2013.
[10] D. Hong, S. Bai, S. M. Lukic, "Closed form expressions for minimizing total harmonic in 3-phase multilevel converters," *IEEE Trans. on Power Electronics*, vol. 29, 2014, d.o.i. 10.1109/TPEL.2013.2290377.
[11] D. Dujic, M. Jones, E. Levi, "Analysis of output current ripple RMS in multi-phase drives using polygon approach," *IEEE Trans. on Power Electronics*, vol. 25, no. 7, pp. 1838-1849, 2010.
[12] D. Jiang, F. Wang, "General current ripple prediction method for multiphase voltage source converters," *IEEE Trans. on Power Electronics*, vol. 29, no. 6, pp. 2643-2648, 2014.
[13] A. Ruderman, B. Reznikov, S. Busquets-Monge, "Asymptotic time domain evaluation of a multilevel multiphase PWM converter voltage quality," *IEEE Trans. on Industrial Electronics*, vol. 60, no. 5, pp. 1999-2009, 2013.
[14] A. Ruderman, B. Reznikov, "Time domain evaluation of filterless grid-connected multilevel PWM converter voltage quality," in *Proc. IEEE Int. Symposium on Industrial Electronics ISIE*, Bari, Italy, 2010, pp. 2940-2945.
[15] A. Ruderman, B. Reznikov, "PWM power converter voltage quality bounds and their applicability to non-PWM control schemes," in *Proc. Int. Conf. Optimization of Electrical and Electronic Equipment OPTIM*, Brasov, Romania, 2010, pp. 618-624.
[16] A. V. Oppenheim, A. S. Willsky, H. S. Nawab, "*Signals and systems*," 2nd ed., Prentice Hall Press, Upper Saddle River, NJ, 1997.
[17] A. V. Oppenheim, R. W. Schafer, "*Discrete-time signal processing*," 3rd ed., Prentice Hall Press, Upper Saddle River, NJ, 2009.
[18] G. Carrara, S. Gardella, M. Marchesoni, R. Salutari, G. Sciutto, "A new multilevel PWM method: a theoretical analysis," *IEEE Trans. on Power Electronics*, vol. 7, no. 3, pp. 497-505, 1992.
[19] E. Levi, D. Dujic, M. Jones, G. Grandi, "Analytical determination of DC-bus utilization limits in multiphase VSI supplied AC drives," *IEEE Trans. on Energy Conversion*, vol. 23, no. 2, pp. 433-443, 2008.
[20] M. Calais, L. J. Borle, V. G. Agelidis, "Analysis of multicarrier PWM methods for a single-phase five level inverter," in *Proc. IEEE Power Electronics Specialists Conf. PESC*, Vancouver, BC, Canada, 2001, pp. 1351-1356.
[21] J. Allmeling, W. Hammer, "PLECS - User Manual," Version 3.3 ed. vol. 2013, 2012.

Obrad Dordevic (S'11, M'13) received his Dipl. Ing. degree in Electronic Engineering from the University of Belgrade, Serbia, in 2008. He joined Liverpool John Moores University in December 2009 as a PhD student. Dr Dordevic received his PhD degree in April 2013 and is now a Lecturer at the Liverpool John Moores University. His main research interests are in the areas of power electronics, electrostatic precipitators, and advanced variable speed drives

Martin Jones (M'07) received his BEng degree in Electrical and Electronic Engineering (First Class Honors) from the Liverpool John Moores University, UK in 2001. He has been a research student at the Liverpool John Moores University from September 2001 till Spring 2005, when he received his PhD degree. Mr Jones was a recipient of the IEE Robinson Research Scholarship for his PhD studies and is currently with Liverpool John Moores University as a Reader.

Emil Levi (S'89, M'92, SM'99, F'09) received his M.Sc. and PhD degrees from the University of Belgrade, Yugoslavia in 1986 and 1990, respectively. He joined Liverpool John Moores University, UK in May 1992 and is since September 2000 Professor of Electric Machines and Drives. He served as Co-Editor-in-Chief of the IEEE Trans. on Industrial Electronics from 2009 till 2013 and is at present an Editor of the IEEE Trans. on Energy Conversion, and Editor-in-Chief of the IET Electric Power Applications. Emil is the recipient of the Cyril Veinott award of the IEEE Power and Energy Society for 2009.